

# Ultrafast All-Optical Analog-to-Digital Conversion using Fiber Nonlinearity

Ken-ichi Kitayama<sup>1)</sup>, Yuji Miyoshi<sup>1)</sup>, Seiji Takagi<sup>1)</sup>, Shu Namiki<sup>2)</sup>

<sup>(1)</sup> Osaka University, kitayama@comm.eng.osaka-u.ac.jp

<sup>(2)</sup> National Institute of Advanced Industrial Science and Technology

**Abstract** Feasibility toward tera-sample/s all-optical ADC using NOLM and its promising applications such as front-end processor of EDC for above 100Gbit/s optical transmission systems are discussed. Recent record-breaking experimental demonstrations of 5-bit ADC will be presented.

## Introduction

Ultrafast analog-to-digital conversion (ADC) will find a wide variety of applications in the near future, including a front-end of digital signal processing (DSP) in optical communications<sup>1</sup>. In conventional electronic ADC, a high resolution at the sampling rate over 100 Giga-samples per second (GS/s) may be difficult due to timing jitter and limited bandwidth of comparator<sup>2</sup>. There has been a real-time 100 GS/s optical sampling that uses four 25 GS/s electronic ADCs in parallel.<sup>3</sup> However, this approach would be difficult to scale to TS/s regime.

We have proposed an ultrafast all-optical quantization and encoding technique using nonlinear optical loop mirrors (NOLM)<sup>4</sup>. In Fig.1 the effective number of bit (ENOB) is plotted against signal bandwidth, which can push the limit to terahertz regime. The all-optical ADC, characterized quantizing and encoding as well as sampling in optical domain, can push the limit to terahertz regime. This is due to the facts that the low-jitter light source is readily available, and optical quantizing based upon fiber nonlinearity will be almost free from bandwidth limitation. Indeed, high temporal resolutions (< 1 ps) and low timing-jitters (< 100 fs) are available by optical sampling techniques with mode-locked laser technology.

In this paper, we will review present status our proposed all-optical ADC. A highlight is a recent record-breaking experimental demonstration of 5-bit ADC<sup>5</sup>. We will also discuss a promising applications, including Tera-Hertz real-time waveform digitizer and a front-end processor for electrical dispersion compensation (EDC) in beyond 100Gbit/s optical fiber transmission systems.

## Principle of operation principle

Figure 2 shows a block diagram of our all-optical ADC. This ADC has one optical input port for input optical analog signal and N outputs for N-bit optical digital signal and signal and consists of an optical sampler and M optical quantizers and encoders consisting of N NOLMs, constructed with HNLF and a 3dB coupler. The analog signal with the time varying optical intensity waveform is sampled by optical sampling techniques with time-interleaving. The sampled optical analog signal is launched into NOLM as a control pulse, while the probe pulse is launched from the arm of the 3dB coupler from the l.h.s.. It propagates

counter-clockwise along with the probe pulse and encounters the clockwise probe pulse. As the intensity of control pulse is much higher, it induces the cross-phase modulation to the counter-clockwise probe pulse. As a result, the fraction of probe pulse appears to the r.h.s. as a function of the intensity of control pulse. This optical input-output transfer function is characterized by a sinusoidal waveform and acts as a quantizer. Noteworthy is that generated code is characterized as Gray Code, which only 1-bit differs from the adjacent codes. Five NOLMs having transfer functions with different number of periods of  $0.5(=2^{1-2})$ , 1, 2, 4, 8 ( $=2^{5-2}$ ) periods are used for 5-bit quantizing and encoding.

## Target operation: 5-bit and sub-TS/s ADC

Key issues below have to be solved;

- #1: Walk-off between control pulse, sampled analog signal and co-propagating probe clock pulse
- #2: Counter-propagation effect, undesired XPM between the control pulse and counter-clockwise probe pulse
- #3: Unwanted SPM caused by the control pulse which causes the spectral overlap between the control and probe pulses as well as unwanted Raman amplification of probe pulse
- #4: Polarization state mismatch between control pulses and probe pulses, which induces deformation in the profile of multi-period optical

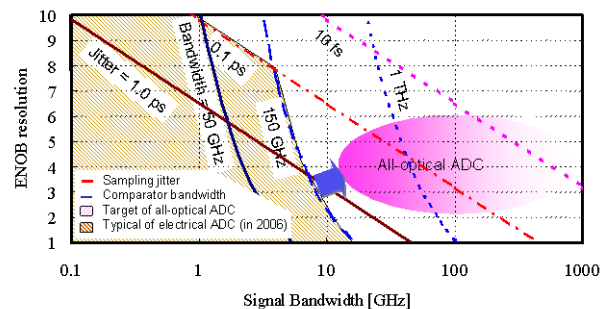


Fig.1 Limitation of resolution

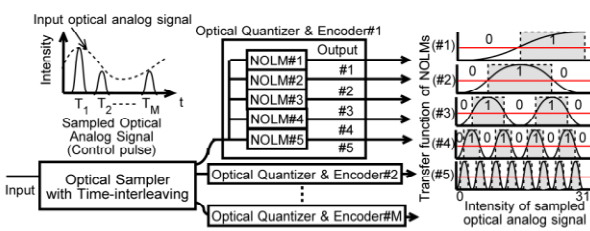


Fig.2 All-optical quantizing and encoding (5-bit)

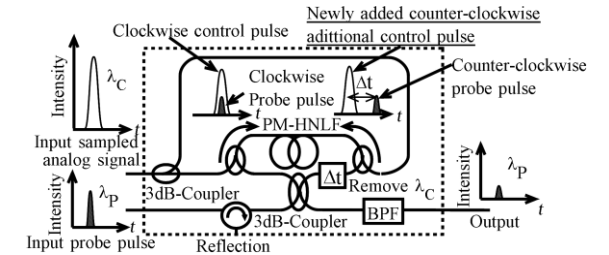
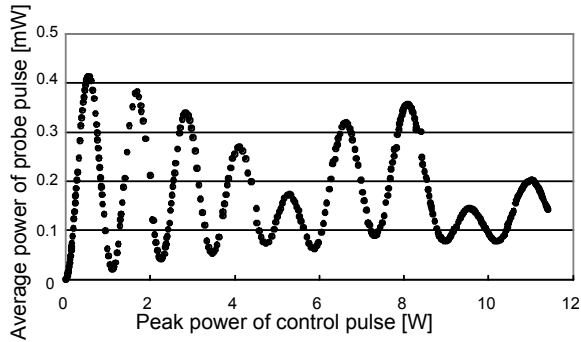
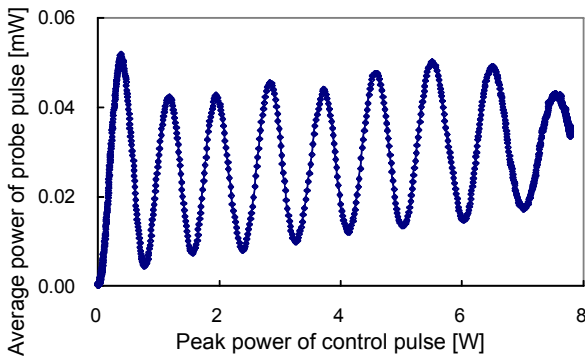


Fig. 3 PM-NOLM with dynamic counter-propagating effect compensation



(a) Non-PM-NOLM



(b) PM-NOLM

Fig.4 8-period optical transfer functions

transfer function of NOLM

We have recently introduced a novel polarization-maintaining (PM)-NOLM with dynamic counter-propagating effect compensation shown in Fig.3. Hence, problems due to the counter-propagation effect (#2) and the polarization mismatch (#4) are readily solved. PM-HNLF has its zero dispersion wavelength  $\lambda_0 = 1568 \text{ nm}$ , the dispersion slope  $D_s = 0.021 \text{ ps/km}^{-1} \text{ nm}^{-1}$ , the fiber loss  $\alpha = 2.7 \text{ dB/km}$ , the nonlinear coefficient  $\gamma = 11.0 \text{ W}^{-1} \text{ km}^{-1}$ , and the length  $L = 0.5 \text{ km}$ . The wavelengths of the control and probe pulses are assigned at 1548nm and 1578nm, respectively so as to mitigate the walk-off effect (#1) and unwanted spectral overlap (#3). The pulsewidths of control and probe pulses are 4.75ps and 2.76ps, respectively. A well-defined 8-period optical transfer function as shown in Fig.4(b) guarantees a record-breaking 5-bit operation at the rate up to 50GS/sec as shown in Fig.7. The sampling rate can be sped up by managing ISI between the control pulses. By contrast, in non-PM-NOLM the offset from ideal transfer function is fatal as shown in Fig.4(a).

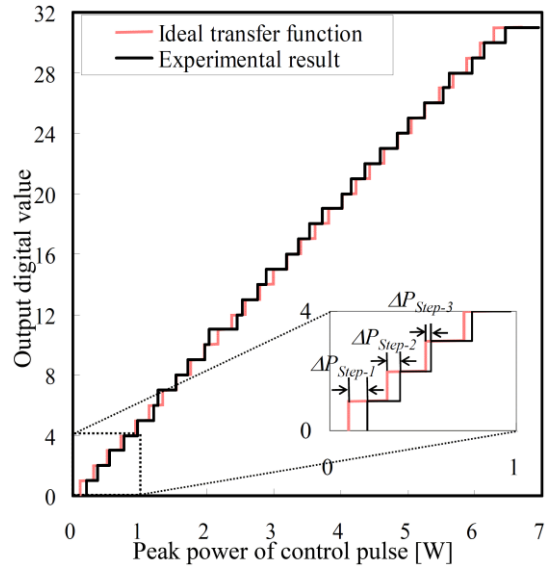


Fig.5 Transfer function of all-optical 5-bit A/D conversion

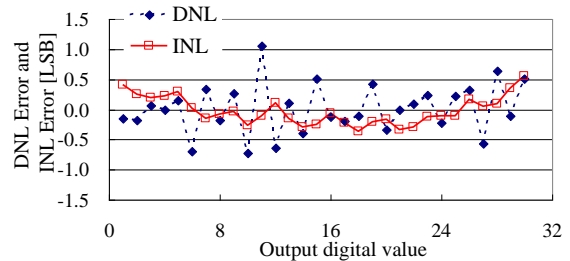


Fig.6 Differential nonlinear error (DNL) and integral nonlinear error (INL)

The transfer functions of all-optical ADC with the adjustments are shown in Fig.5. The relative power ratio of five NOLMs is determined to be 1/16.4 : 1/8.48 : 1/4.30 : 1/2.11 : 1 from the most significant bit (MSB) to the least significant bit (LSB). Note that the power ratio should be 1/16, 1/8, 1/4, 1/2, and 1 for the ideal profile of multi-period transfer function. Figure 5 shows that the transfer function monotonically increases with no missing-code performance. Figure 6 shows a peak differential nonlinearity (DNL) error and the integral nonlinearity (INL) error. The peak DNL error of 1.06 LSB, and the maximum INL error is 0.56 LSB.  $-1 < \text{INL} < 1$  and  $\text{DNL} > -1$  indicate a good precision by the standard of electronic ADC.

The ENOB is of the most importance, representing the resolution of ADC. The ENOB of this all-optical ADC equivalent to conventional electronic ADC is calculated as

$$\begin{aligned}
 ENOB &= \frac{20 \log \left( \frac{R_{Load} \times R_{PD} \times P_{Opt-S}}{R_{Load} \times R_{PD} \times P_{Opt-N}} \right) - 1.76}{6.02} \quad (1) \\
 &= \frac{20 \log \left( \frac{P_{Opt-S}}{P_{Opt-N}} \right) - 1.76}{6.02}
 \end{aligned}$$

where  $P_{Opt-S}$  and  $P_{Opt-N}$  are signal and noise power root-mean-square of optical signal without DC component, respectively.  $R_{Load}$  and  $R_{PD}$  are the load resistance and the responsivity of the PD, respectively.

The signal power and quantization noise with nonlinear error  $\Delta P_{Step-i}$  can be written by

$$P_{Opt-S} = \frac{P_{FS}}{2\sqrt{2}},$$

$$P_{Opt-N} = \sqrt{\frac{1}{12} \left(\frac{P_{FS}}{2^N}\right)^2 + \frac{1}{2^N} \sum_{i=1}^{2^N-1} (\Delta P_{Step-i})^2} \quad (2)$$

where  $P_{FS}$  is full-scale of power range. N is the number of bit resolution of ADC. Its ENOB of calculated transfer function is 4.41 bit. The degradation of ENOB is estimated only 0.59 bit, resulting in the ENOB of 4.41 bit. All-optical ADC is characterized a high ratio of ENOB and its designated resolution, 4.41/5, compared with the value well below unity, for example 5/8, of the electronic counter part.

**Novel applications**

**A. Tera-Hertz Real-time Waveform Digitizer**

1TS/s optical real-time digitizer can be constructed by optical time-interleaving by using 20 5-bit optical quantizers and encoders at 50GS/s. For a demonstrator, all-optical 4-bit ADC using 16-fold optical time-interleaving at the sampling rate of 160 GS/s has been successfully demonstrated [4]. Figure 7 compares the measured waveform of an input analog signal and 32 output digital signals (4 bits x 8 of 16 timeslots) at 160GS/s. Figure 8 shows the input analog signal and output digital values at 288 sampling points. In optical sampling techniques,

**B. Beyond 100Gbps Frontend processor for EDC**

Another promising application is a front-end processor of EDC. An ADC with the ENOB of 4.41 might not be high enough but could be applicable for 100Gbit/s optical multi-level modulation formats such as 25Gsymbol/s Pol-mux QPSK. Compared with conventional electronic ADC in a parallel configuration as shown in Fig.9, advantages include a single optical ADC without serial-to-parallel converter.

**Conclusions**

A review of all-optical ADC highlighting a recent record-breaking experimental demonstration of 5-bit ADC has been presented. Promising applications to tera-Hertz real-time waveform digitizer and a front-end processor for electrical dispersion compensation (EDC) in beyond 100Gbit/s optical fiber transmission systems have been discussed.

**Acknowledgments**

The authors would like to thank K. Kokura and R. Sugisaki of Furukawa Electric for providing PM fibers and H. Nagaeda of Trimatiz for his cooperation in the experiments.

**References**

- 1 H.F. Haunstein, et al., IEEE/OSA J. Lightwave Technol. **22**, 1169 (2004).
- 2 G. C. Vally, Opt. Express **15**, 1955 (2007)

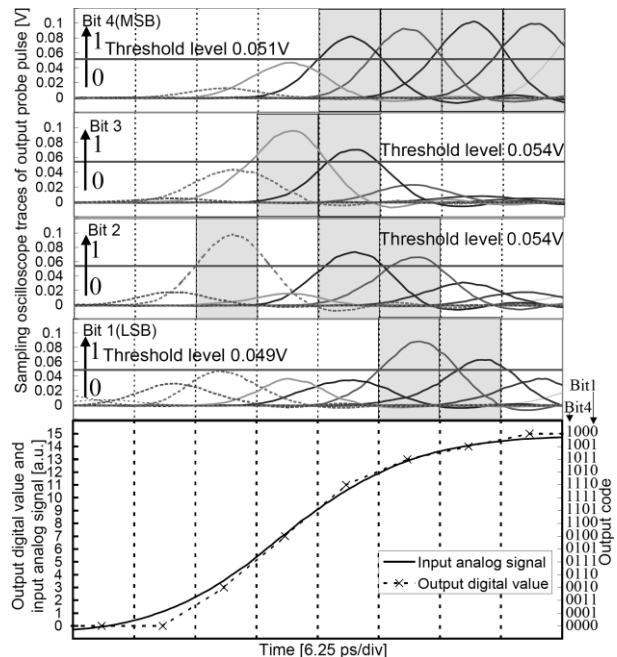


Fig.7 Measured waveforms of each timeslot and output digital value

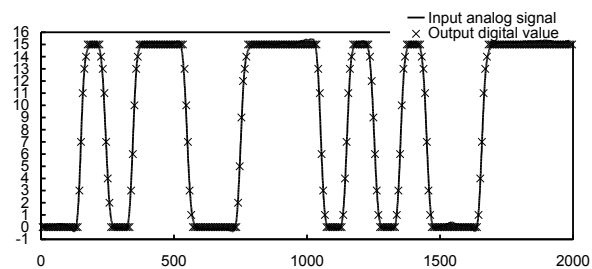


Fig.8 160Gbit/s digitized waveform (288 sampling points)

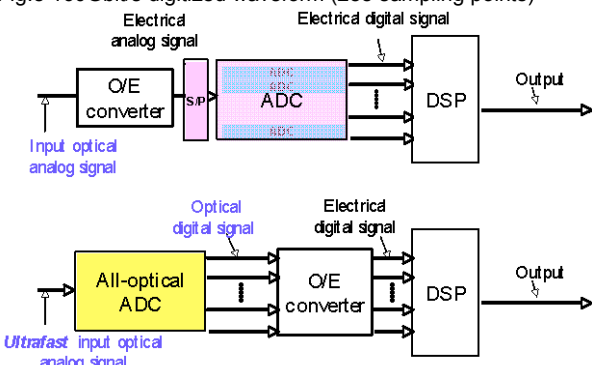


Fig.9 All optical ADC vs. electronic ADC

- 3 M.Skold, et al., ECOC 2007, PD1.1 (2007).
- 4 K. Ikeda et al., IEEE/OSA J. Lightwave Technol. **26**, 2618 (2006).
- 5 Y. Miyoshi, et al., OFC 2009, PDPA6 (2009).